PROCESSING CHALLENGES FOR GaN-BASED PHOTONIC AND ELECTRONIC DEVICES

S.J. Pearton *, F. Ren **, R.J. Shul ***, J.C. Zolper *** and A. Katz ****
* Department of Materials Science and Engineering, University of Florida, Gainesville, 32611
** Bell Laboratories, Lucent Technologies, Murray Hill, NJ 07974
*** Sandia National Laboratories, Albuquerque, NM 87185
**** EPRI, Palo Alto, CA 94304

ABSTRACT

The wide gap materials SiC, GaN and to a lesser extent diamond are attracting great interest for high power/high temperature electronics. There are a host of device processing challenges presented by these materials because of their physical and chemical stability, including difficulty in achieving stable, low contact resistances, especially for one conductivity type, absence of convenient wet etch recipes, generally slow dry etch rates, the high temperatures needed for implant activation, control of suitable gate dielectrics and the lack of cheap, large diameter conducting and semi-insulating substrates. The relatively deep ionization levels of some of the common dopants (Mg in GaN; B, Al in SiC; P in diamond) means that carrier densities may be low at room temperature even if the impurity is electrically active - this problem will be reduced at elevated temperature, and thus contact resistances will be greatly improved provided the metallization is stable and reliable. Some recent work with $CoSi_x$ on SiC and W-alloys on GaN show promise for improved ohmic contacts. The issue of unintentional hydrogen passivation of dopants will also be covered - this leads to strong increases in resistivity of p-SiC and GaN, but to large decreases in resistivity of diamond. Recent work on development of wet etches has found recipes for AlN (KOH), while photochemical etching of SiC and GaN has been reported. In the latter cases p-type materials is not etched, which can be a major liability in some devices. The dry etch results obtained with various novel reactors, including ICP, ECR and LE4 will be compared - the high ion densities in the former techniques produce the highest etch rates for strongly-bonded materials, but can lead to preferential loss of N from the nitrides and therefore to a highly conducting surface. This is potentially a major problem for fabrication of dry etched, recessed gate FET structures.

INTRODUCTION

There is an increasing interest in use of compound semiconductors for several high power/high temperature solid state devices for applications in power electronics, control and distribution circuits, hybrid drive-train automobiles, "more electric" aircraft (avionics) and next generation battleships [1-10]. The three major commercial markets for these devices are automotive, industrial factories and electric utility, while numerous tri-service defense applications also require high power heat tolerant devices. Typical device characteristic requirements for many of the existing and emerging applications are: high voltage (600-1000 V), low switching losses, high current densities (1000 A/cm^2), and operating temperatures up to 350°C. While silicon, and to a much lesser extent GaAs have been used for power devices, SiC and emerging materials such as GaN have significant advantages because of wider bandgaps (higher operating temperature), larger breakdown fields (higher operating voltage), higher electron saturated drift velocity (higher operating current) and better thermal conductivity (higher power density). Some of the properties important for power device applications for GaN, SiC

and Si are listed in Table I. The basic building blocks of SiC and GaN power technology are gate-turn off thyristors (GTOs), insulated gate bipolar transistors (IGBTs), and metal-oxide semiconductor controlled thyristors (MTOs). The superior device performance of compound semiconductors can be exemplified by a SiC MOS turn-off thyristor (MTO) which can carry three times higher current, and possesses eight times higher breakdown voltage than a comparable Si MTO [1]. In addition, SiC MOS MTOs can operate at much higher temperatures (250°C for SiC vs. 125°C for Si).

There are several key issues that must be addressed to fully exploit the thyristor type devices in both SiC and GaN [9]. These are:

(i) Improvement of gate oxide quality;
(ii) Better edge termination and passivation process;
(iii) Improved ohmic contacts;
(iv) Higher implant activation efficiencies and damage removal;

For GaN-based photonic devices there are also a number of critical advances necessary in:

(i) p-contact technology;
(ii) Mesa facet quality and yield;
(iii) Layer structure design and control.

In this paper we will show some of the recent advances in process technology for wide bandgap materials and suggest directions for future research.

Table I: High Temperature Power Devices: Potential Candidates

	Material		
Property	Si	3C SiC (6C SiC)	GaN
Bandgap	1.1	2.2 (2.9)	3.4
Maximum Operating temperature (K)	600	1200 (1580)	?
Melting Point (K)	1690	sublimes>2100?	>2200
Physical Stability	Good	Excellent	Good
Hole Mobility (RT, cm^2/Vs)	600	40	150
Electron Mobility (RT, cm^2/Vs)	1400	1000 (600)	900
Breakdown Voltage (Eb, 10^6 V/cm	0.3	4	5
Thermal Conductivity (C_T, W/cm)	1.5	5	1.3
Saturation Electron Drift Velocity (cm/s)	$1x10^7$	$2x10^7$	$2.7x10^7$
Dielectric Constant (K)	11.8	9.7	9

OMIC CONTACTS

For SiC, recent advances in epilayer growth have provided more highly-doped (Al) p-type layers for improved ohmic contacts. Much of the work involved Al-based metallization with contact resistivities of 10^{-4}-$10^{-5}\Omega cm^2$, with relatively poor thermal stability [12]. The best contact properties were obtained for samples annealed at 800-1000°C for 5 mins. Lundberg and Ostling [13] reported $CoSi_2$ ohmic contacts with ρ_c <$4x10^{-6}\Omega cm^2$ to p-type SiC, fabricated using sequential evaporation and a 2-step anneal at 500/900°C. The silicidation process of simple Co/SiC contacts reduced the sheet resistance under the contact pads significantly. On lightly-doped SiC, the $CoSi_2$ produced barrier heights of 1.05 eV (n-type) and 1.90 eV (p-type), but on heavily doped material (doping ≥$10^{19}cm^{-3}$), ρ_c values of $3x10^{-5}\Omega cm^2$ (n-type) and $4x10^{-6}\Omega cm^2$ (p-type) were obtained [14].

DISCLAIMER

Some novel W-based Schottky contacts based on W and WC on SiC have also been reported [14]. Chemically vapor deposited (400°C) W produced ϕ_B values of 0.79 eV on n-type material, and 1.89 eV for p-type SiC. WC films deposited by CVD from $WF_6/C_3H_8/H_2$ mixtures at 900°C produced ϕ_B values of 0.89 eV (n-type) and 1.81 eV (p-type), with little deterioration after 6 hr at 500°C for the latter.

Ren [15] has recently reviewed ohmic contracts to III-nitrides. The use of degenerately n-type InN [16] or creation of InN by N^+ ion bombardment of InP [17] produces specific contact resistivities $<10^{-6}\Omega cm^2$ with nonalloyed TiPtAu metallization.

Lin et al. [18] have obtained extremely good ohmic contacts on n-type GaN layers grown on sapphire substrates. Using Ti/Al metallization scheme they were able to obtain specific contact resistivies as low as $8x10^{-6}\Omega cm^2$ after annealing at 900°C for 30 sec This investigation also involved a materials study which linked the low contact resistance to the formation of a TiN_x interfacial phase.

It is reported that Ti/Al metallization on unintentional doped n-GaN ($1x10^{17}cm^{-3}$) showed linear I-V characteristics for small current levels (300μA). After the 500°C RTA anneal, the contact resistance of $10^{-3}\Omega$-cm^2 was obtained.[18] Upon further annealing at 900°C for 30 sec. The contact resistance was reduced to $8x10^{-6}\Omega cm^2$. The annealing time for 900°C annealing also played an important role. After annealing at 900°C for 20 sec, the Al and Ti diffraction peaks were absent from the XRD data as compared to the as-deposited sample. New peaks were observed and identified as face-center-tetragonal TiAl. AES depth profile of the annealed sample also showed that the metal/GaN interface (150 Å) was not completely abrupt. It is believed that this interface is essential for the formation low resistance ohmic contacts. During the 900°C anneal, the N diffused out from GaN and reacted with Ti to form TiN. Thus, N vacancies were created right at the metal GaN interface. Since N vacancies in GaN act as donors, this interface region would become a heavily doped n-GaN layer and provide low resistance contact formation. However, TEM analysis will be needed to confirm the reactions between TiAl and GaN. The reason for high contact resistance after annealing for 60 sec was speculated as the oxygen incorporated into the Al layer and formed a thin insulating Al_2O_3 layer on the surface of metallization. This caused the error for the contact resistance measurement.

Au/Ti metallization on GaN was also studied along with Al/Ti metallization. The as-deposited samples showed higher specific contact resistivity around $10\text{-}10^{-1}\Omega cm^2$. After annealing at 700°C, it improved to $10^{-2}\text{-}10^{-3}\Omega cm^2$ range. However, after further annealing at 900°C for 30 sec, the contact resistance increased substantially. The cause of this increase was not explored.

Lin et al. demonstrated a novel ohmic contact scheme to GaN using an InN/GaN short-period superlattice (SPS) and an InN cap layer [19]. A ten-period 0.5 nm/0.5 nm InN/GaN SPS structure was grown on a 0.6μm GaN with a 5 nm thick InN cap layer. The doping level for the n-GaN in the channel and SPS is around $5x10^{18}cm^{-3}$. The doping level of n-InN cap layer and SPS was about $1x10^{19}cm^{-3}$. Contact metallization consisted of 20 nm Ti and 100 nm Al. From TLM data, the specific contact resistance was $6x10^{-5}\Omega$-cm^2. Thermal annealing at temperature below 500°C led to no significant change in the contact resistivity. In this case, electrons tunnel through the SPS conduction band, effectively reducing the potential barrier formed by the InN/GaN heterostructure leading to lower contact resistances.

Generally Au/Ti contacts suffer from the problem of spiking into the underlying semiconductor upon annealing and have large contact resistance after thermal annealing, as described in previous section. To mitigate this problem, Pt which is a very good diffusion barrier has been used between Ti and Au to prevent Au spiking [20].

W was found to produce low specific contact resistance (ρ_c~$8.0x10^{-5}\Omega$-cm^2) ohmic contacts to n^+-GaN ($n=1.5x10^{19}cm^{-3}$) with limited reaction between the metal and semiconductor up to 1000°C. The formation of the β-W_2N and W-N interfacial phases were deemed responsible for the electrical integrity observed at these annealing temperatures. No Ga out-diffusion was observed on the surface of thin (500Å) W contacts even after 1000°C, 1 min anneals. Thus, W appears to be a stable contact to n^+-GaN for high temperature applications [21].

The unintentional doping levels of MOMBE grown $In_xGa_{1-x}N$ and $In_xAl_{1-x}N$ are very dependent on the In composition [22]. For the case of $In_xGa_{1-x}N$, the doping level of $In_xGa_{1-x}N$ is as high as $10^{20}cm^{-3}$ for a wide range with x (In ratio) larger than 0.37. For $In_xGa_{1-x}N$ with such high doping levels, nonalloyed ohmic contacts can be achieved. With the increase of In concentration in $In_xGa_{1-x}N$, it will also lower the bandgap of InGaN which will further reduce the contact resistance. These $In_xGa_{1-x}N$ layers were proposed for W contacts as ohmic contact layer on GaN and specific contact resistivities as a function of annealing temperature are shown in Figure 1. The contact resistance of as deposited samples is realized as low as $7x10^{-6}\Omega cm^2$.

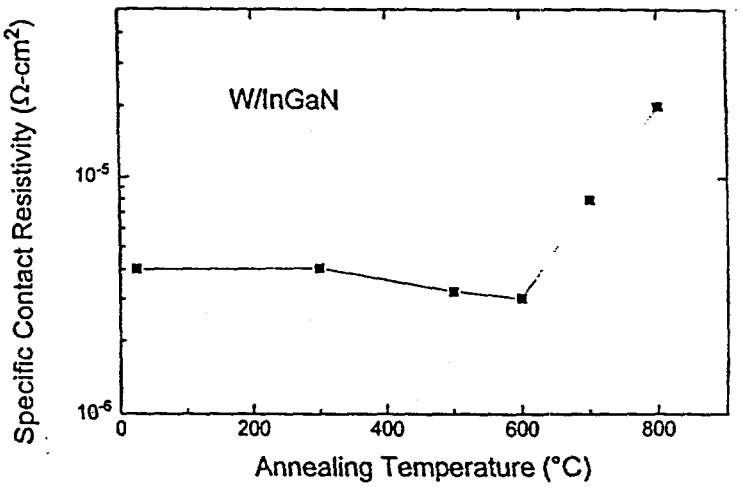

Figure 1. Specific contact resistivity of W/InGaN as a function of annealing temperature [15].

Processing of implanted devices involves a high temperature annealing step for implant activation, typically >700°C. The stability of the WSi_x/InGaN contacts are essential to allow the high temperature process for dopant activation. The contact degradation at higher annealing temperature was related to increases in the sheet resistance, which resulted from the degradation of the metal-semiconductor interface.

From SEM studies, the as-deposited sample exhibited a very smooth surface and there was no change in the surface morphology of samples annealed at temperatures of 400 and 700°C [20]. The surface morphology of the samples annealed at 900°C showed only a small amount of surface roughness. The maximum annealing temperature to obtain good surface morphology WSi_x contacts on InGaN samples would therefore be in the range of 700-800°C. The AES studies generally confirmed the SEM observation regarding the inert nature of the metal-semiconductor interface, but indicated interdiffusion of various elements as a result of RTA at temperature of 900°C.

As shown in Figure 2, the specific contact resistivities of as-deposited W on $In_{0.6}Al_{0.4}N$ in which the unintentional doping level is $10^{18}cm^{-3}$ is in the high $10^{-4}\Omega$-cm^2 range [23]. Although the contact resistance reduces to $7x10^{-4}\Omega$-cm^2 after annealing up to 500°C, it is still quite high for device applications. Since the unintentional doping level of InN is two orders of magnitude higher than that of $In_{0.6}Al_{0.4}N$, InN with a graded $In_xAl_{1-x}N$ layer can be used as a contact layer

for InAlN devices: As illustrated in Figure 3, the contact resistance of W/InN/graded-$In_xAl_{1-x}N$/InAlN is half of that for W/InAlN, and the thermal stability is also improved. The contact morphology and resistance show no degradation up to 500°C. AES depth profiles of W/InN/graded-$In_xAl_{1-x}N$/InAlN samples showed there was only slight differences between as-deposited and 500°C annealed material. It was suggested that nitrogen diffused out into the contact metallization and formed on interfacial WN_2 phase, which improved contact resistance. Both morphology and ρ_c degraded at higher annealing temperature.

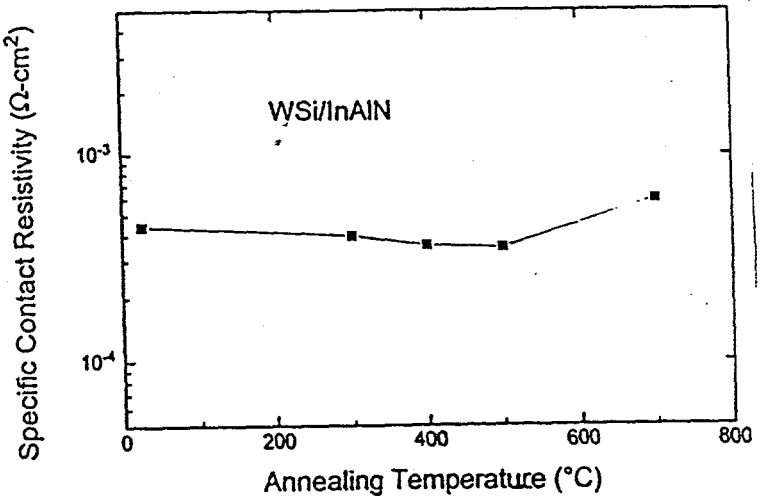

Figure 2. Specific contact resistivity of WSi_x/InAlN as a function of annealing temperature [15].

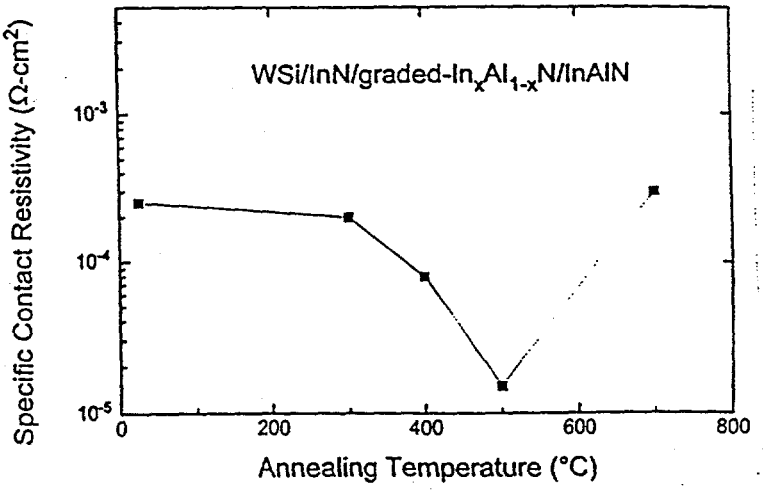

Figure 3. Specific contract resistivity of WSi_x/InN/graded $In_xAl_{1-x}N$/InAlN as a function of annealing temperature.

Several groups have reported improved ohmic contact properties for Ti/Al [26] or TiAlNiAu [27] on n-GaAs on which the surface was made more conducting by loss of N, either by annealing [26] or reactive ion etching [27]. Depth profiles of Ti/Al contacts annealed at 400°C showed that low contact resistance was only achieved after Al diffused to the GaN interface, suggesting a Al-Ti intermetallic is responsible for the improved properties [28]. Another intermetallic compound, $PtIn_2$, has also been used for ohmic contacts to n-GaN, and it was suggested that formation of InGaN at the interface was necessary [29].

Far less work has been done with contacts to p-GaN, where Ni/Au is the standard metallization for laser and light-emitting diodes.[30] No metallization has been found that produces the desirably low ρ_c of $<10^{-6}\Omega$-cm^2.

Much progress has recently been made in the areas of growth, dry etching, implant isolation and doping of the III-V nitrides and their ternary alloys. This has resulted in nitride-based blue/UV light emitting and electronic devices [31-39]. There has been less success in developing wet etch solutions for these materials, due to their excellent chemical stability. High etch rates have been achieved in dry etch chemistries [40-49], but damage may be introduced by ion bombardment, and controlled undercutting is difficult to attain. In addition, since dry etching has a physical component to the etch, selectivities between different materials is generally reduced.

Amorphous AlN has been reported to etch in 100°C HF/H_2O [50-52], HF/HNO_3 [53], and NaOH [54], and polycrystalline AlN in hot (≤85°C) H_3PO_4 at rates less than 500Å/min [55,56]. Mileham et al. [57] reported the etching of AlN defective single crystals in KOH based solutions at etch temperatures ranging from 23 to 80°C. They reported decreased etch rates with increasing crystal quality, as the reactions occurred favorably at grain boundaries and defect sites. InN in aqueous KOH solutions was reported to etch a few hundred angstroms per minute at 60°C [58].

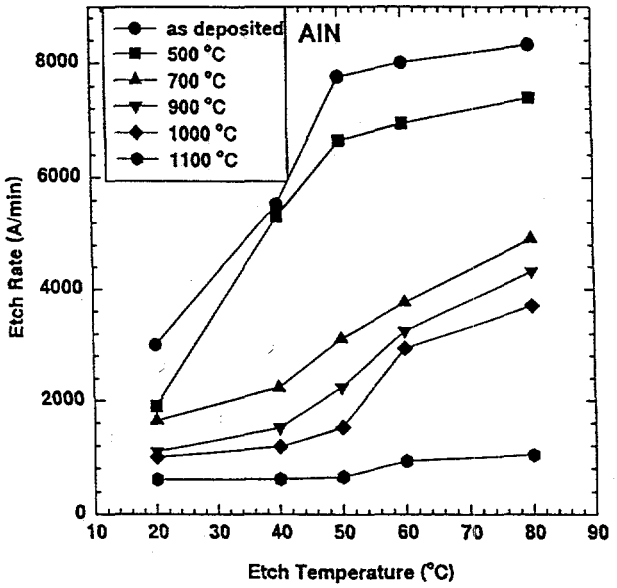

Figure 4. Etch rate of AlN in KOH solutions as a function of etch temperature for samples as-deposited or annealed at 500, 700, 900, 1000, and 1100°C.

Wet chemical etching of AlN and $In_xAl_{1-x}N$ was investigated in KOH-based solutions as a function of etch temperature and material quality [59]. The etch rates for both materials increased with increasing etch temperatures, which was varied from 20 to 80°C. The crystal quality of AlN prepared by reactive sputtering was improved by rapid thermal annealing at temperatures to 1100°C with a decreased wet etch rate of the material measured with increasing anneal temperature [Figure 4]. The etch rate decreased approximately an order of magnitude at 80°C etch temperature after an 1100°C anneal. The etch rate for $In_{0.19}Al_{0.81}N$ grown by metallorgainc molecular beam epitaxy was approximately three times higher for material on Si than on GaAs. This corresponds to the superior crystalline quality of the material grown on GaAs. Etching of $In_xAl_{1-x}N$ was also examined as a function of In composition. The etch rate initially increased as the In composition changed from 0 to 36%, and then decreased to 0 Å/min for InN [Figure 5]. We also compared the effect of doping concentration on etch rate. Two

InAlN samples of similar crystal quality were also etched; one was fully depleted with n $<10^{16}cm^{-3}$ (2.6% In) and the other n~$5x10^{18}cm^{-3}$ (3.1% In). At low etch temperature, the rates were similar, but above 60°C the n-type sample etched faster, approximately three times faster at 80°C. The activation energy for these etches is very low, 2.0 ± 0.5 kcal mol^{-1} for sputtered AlN. The activation energies for InAlN were dependent on In composition and were in the range 2 to 6 kcal Mol^{-1}. GaN and InN layers did not show any etching in KOH at temperatures up to 80°C.

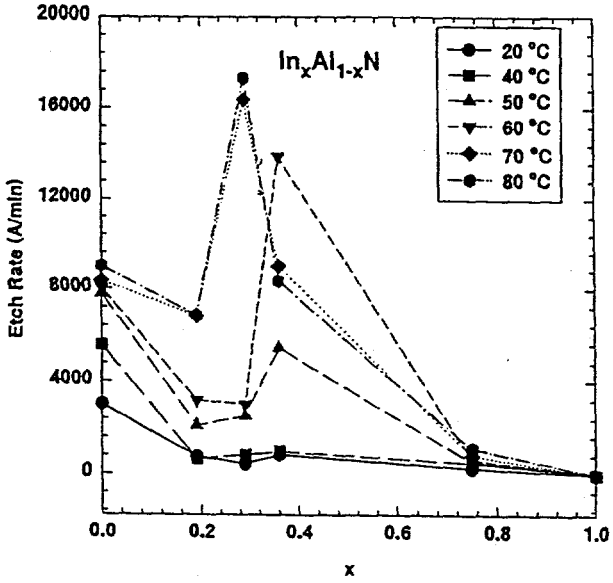

Figure 5. Etch rate for $In_xAl_{1-x}N$ for $0 \leq x \leq 1$ at KOH solution temperatures between 20 and 80°C.

Minsky et al. [60] demonstrated photo-electrochemical etching of GaN under illumination by a He-Cd (d=325 nm) laser using KOH and HCl solutions. Annealed (900°C) Ti contacts were used as electrical contacts and etch masks. Broad area photo-electrochemical etching of n-type β-SiC has previously been reported [61], and the same technique has been applied to n-GaN [62], using Hg lamp exposure and unannealed Ti metal contacts. Etch rates of 170-200Å $\cdot min^{-1}$ were obtained for n-type material, but no etching was found for p-type GaN.

DRY ETCHING

The current status of dry etching of nitrides has recently been reviewed by Gillis et al. [63]. The baseline technique employed, reactive ion etching (RIE) produces GaN etch rates of up to 1,000Å $\cdot min^{-1}$ at high dc self-biases (-300 to -400 V). Many plasma chemistries have been used, including those common for III-V semiconductors such as Cl_2, Cl_3, $SiCl_4$, CCl_2F_2, HBr/H_2, CH_4/H_2 and CHF_3. Magnetic enhancement of the discharge, as in magnetron RIE, leads to much larger rates (3000Å $\cdot min^{-1}$ at -100 V self-bias) [64]. The highest etch rates are obtained with high ion density plasma sources such as Electron Cyclotron Resonance (ECR) and Inductively Coupled Plasma (ICP) [45,47-49,65]. Rates up to 1.3μm $\cdot min^{-1}$ for GaN have been obtained with ICl/Ar ECR discharges. The ion energy threshold for the onset of etching GaN and InN is ~75 eV. Surface roughening and N depletion can occur at high ion energies. Little work has been done a systematic damage studies, but initial reports show that nitrides are more resistant to introduction of electrically active point defect damage that other III-V's [66], but that even low ion energy conditions can induce N-deficient surfaces [67] and degradation of luminescence [68].

A promising low damage technique is low energy, electron-enhanced etching (LE4), which avoids ion bombardment altogether [63,69]. LE4 of GaN/Si and GaN/SiC in direct current H_2 and H_2/Cl_2 plasmas has been reported at rates up to 2500Å $\cdot min^{-1}$ [63,69]. Another technique that avoids ion bombardment is photo-assisted vapor etching [70], where GaN has been etched in HCl vapor while being irradiated with an excimer laser and held at 200-400°C.

For SiC, basically all of the pattern steps during device processing must be carried out with dry etching due to the chemical stability and inertness of SiC in conventional acid or base solutions at normal temperatures [71]. Most of the dry etching processes reported to date have employed reactive ion etching (RIE) with chlorofluorocarbon (CHF_3 and related gases) or NF_3, and hydrogen is generally added to the plasma chemistry to avoid rough surfaces [72-75]. Flemish et al. [76-78] and Casady et al. [74] reported that higher ion density Electron Cyclotron Resonance (ECR) discharges of CF_4/O_2 or SF_6/O_2 produced much higher etch rates than RIE, and it was not necessary to add H_2 to the plasma chemistry to obtain smooth surface morphologies. Changes to the electrical quality of Schottky diodes fabricated on the dry etched surfaces were less severe with the ECR discharges [78], and the threshold ion energies for creating damage were also determined. (~100 eV in ECR and ~150 eV in RIE).

In work on other difficult-to-etch materials such as GaN, NiFeCo and SrS we have found that in many cases the etch rates are not limited by the volatility of the etch products, but by the initial bond-breaking that must precede formation of these products. The inherent advantage of ECR discharges over RIE plasmas is the high ion density ($\geq 10^{11} cm^{-3}$ compared to $\leq 10^{9} cm^{-3}$) that aids in the initial bond breaking and subsequent product desorption. We have recently compared different plasma chemistries, including Cl_2, IBr, SF_6 and NF_3, for ECR etching of SiC. All of these chemistries are hydrogen-free and thus avoid any hydrogen passivation of near-surface dopants.

The expected etch products for SiC in Cl_2-based gas chemistries are $SiCl_4$ and CCl_4, both of which have high vapor pressure at room temperature and therefore on would expect reasonably good etch rates. Figure 6 shows the etch rate of SiC in 1000 W ECR discharges of $10Cl_2/5Ar$, as a function of applied rf chuck power. The threshold for observing any etching is ~50 W, with the etch rate linearly dependent on ion energy (which is proportional to rf power). Therefore, even at high ion density (high microwave power) it is necessary to have an ion energy above the threshold for breaking bonds in the SiC. The presence of the Ar^+ ions is very important in this process – we found that the etch rate increased with percentage Cl_2 in the plasma up to ~$10Cl_2$-/5Ar, but decreased rapidly thereafter (to ~500 Å/min in pure Cl_2 plasmas at 150 W rf and 1000 W microwave power). Lower etch rates were obtained with IBr plasma chemistries under the same conditions.

Oxygen has often been added to fluorine-based gas chemistries under RIE conditions to enhance the active fluorine concentration and increase SiC etch rate [76,79]. Under ECR conditions, however we observed little benefit for O_2 addition to either NF_3 or SF_6, as shown in Figure 7. Note that NF_3 produces etch rates roughly three times faster than SF_6 because it is more easily dissociated (bond strength 62.1 kCal/mol compared to 82.9 kCal/mol). There is little change in the intensity of the atomic fluorine lines in the 6000-7000Å region of the optical emission spectra of SF_6 with increasing O_2 content with the SF_x lines at ~4500Å decreasing and the O lines at ~8000Å increasing as expected. The ion energy threshold for the onset of etching is absent with NF_3. We obtained etch rates of ~1100Å/min even at 0V self-bias – the ion energies in this case are what is associated with the ECR plasma generation itself, i.e. ~20 eV. Note again however that the etch rate increased in an almost linear fashion with self-bias, which suggests that the increased efficiency of bond-breaking is a key parameter in determining etch rate. The etched surface morphologies were typically similar to those of the unetched control samples, without the need for H_2 addition.

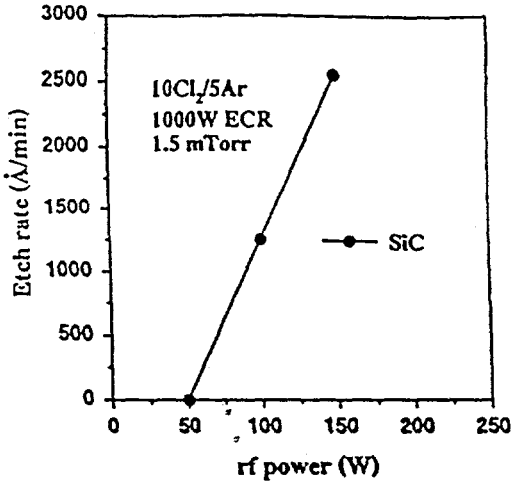

Figure 6. Etch rate of SiC in 1000 W microwave, 1.5 mTorr discharges of $10Cl_2/5Ar$, as a function of rf power.

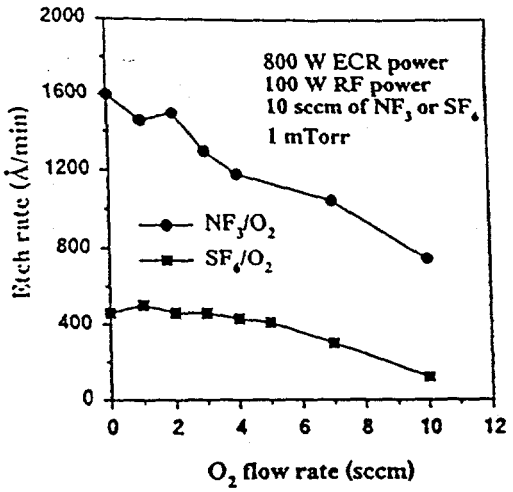

Figure 7. Etch rate of SiC in 800 W microwave, 100 W rf, 1 mTorr discharges of NF_3/O_2 or SF_6/O_2, as a function of O_2 flow rate. Total pressure and flow rate were held constant.

The introduction of dry etch damage into n-type SiC epilayers was measured by monitoring the sheet resistance after exposure to Ar plasmas under both RIE and ECR conditions. In these 1μm thick films, the threshold rf powers for measurable resistance changes were ~250 W (-275 V dc bias) for RIE and ~150 W (-170 W dc bias) for ECR conditions (1000 W microwave power). The SiC is much more resistant to introduction of dry etch damage than Si, as expected from its high bond strength. Significant annealing of the damage introduced by ion bombardment occurred at ~700°C, corresponding to an activation energy for damage removal of ~3.4 eV [80].

Etch rates > 1500Å/min are found for SiC in ECR Cl_2/Ar or NF_3 plasmas with moderate rf bias. There is a threshold rf power for the onset of etching in Cl_2/Ar (~50 W), whereas NF_3 is found to produce etching even with no biasing of the substrate. Addition of O_2 to NF_3 des not produce any significant etch rate enhancement, and addition of H_2 to Cl_2 plasmas greatly retards the SiC etch rate. The etched surfaces retain their original morphology in all of the chemistries we investigated, and small quantities of S-residues are detected on SF_6-etched samples. These

ECR processes appear quite suitable for pattern transfer into SiC at higher rates than obtainable with RIE. Photoresist is in general not a good choice as a mask material since it is readily etched in the chemistries discussed here, and indium tin oxide is a better choice [71].

ION IMPLANTATION/ANNEALING

Several recent studies have established the thermal stability limits of GaN, AlN and InN during both rapid thermal annealing [81] and vacuum annealing [82]. Figure 8 shows the nitrogen desorption rate for these binaries [82]. The effective activation energies for N_2 decomposition in vacuum were 3.48 eV (InN), 3.93 eV (GaN) and 4.29 eV (AlN). These are a factor of approximately 1.7 times higher than the binding energies of a single metal-N bond (respectively 1.93 eV, 2.2 eV and 2.88 eV for InN, GaN and AlN) [83]. The nitrogen flux from the unprotected nitride surfaces peaked at 685°C (InN), 985°C (GaN) and >1120°C (AlN) [82]. Under RTA conditions, loss of nitrogen was found to create then, degenerately n-type surfaces on the binary nitrides, with stability limits of ≤600°C (InN), 800°C ($In_{0.5}Ga_{0.5}N$, $In_{0.75}Al_{0.25}N$), ~1100°C (GaN) and ~1100°C (AlN) [81].

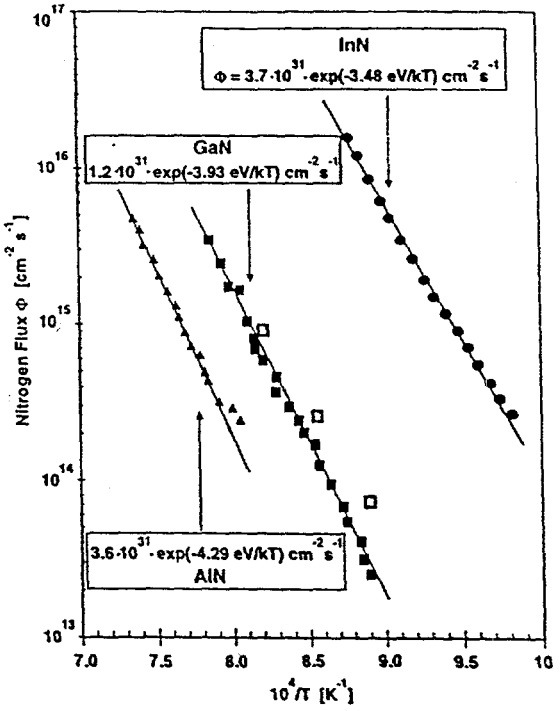

Figure 8. Nitrogen flux or decomposition rate for InN, GaN and AlN in vacuum over the temperature range of decomposition [82].

We have compared use of GaN, InN and AlN powder for providing nitrogen partial pressure within a graphite susceptor during high temperature rapid thermal annealing of GaN, AlN, InN and InAlN. At temperatures above ~750°C vapor transport of In from InN powder produces In droplet condensation on the surface of all nitride samples being annealed. GaN powder provides better surface protection than AlN powders for temperatures up to ~1050°C when annealing GaN and AlN samples. Dissociation of nitrides from the surface is found to occur with approximate activation energies of 3.8 eV, 4.4 eV and 3.4 eV, respectively, for GaN, AlN and InN.

The first reports of the use of ion implantation to introduce impurities into GaN dates back to 1972 with work done by Pankove and coworkers on the photoluminescence of 35 implanted

impurities in GaN [84]. Although luminescence data was given, no electrical data was reported. To remove the implant damage and achieve good luminescence the samples were annealed for 1 hr in flowing ammonia (NH_3). Most likely, hydrogen liberated from the ammonia ambient or hydrogen already grown into the GaN films was responsible for electrically passivating these impurities. This is likely since hydrogen is known to passivate Mg and Ca acceptors in GaN [85-87]. Once the role of hydrogen was understood with respect to passivating epitaxial dopants, primarily acceptors, it was clear that the implantation anneal sequence should also be done in a hydrogen-free ambient.

Other implantation work by Wilson et al. focused on the redistribution properties of potential dopants in GaN [88]. That work demonstrated that, at least up to 900°C, none of the implanted species studied (Be, Mg, Zn, C, Se, Ge) showed measurable redistribution with annealing for times up to 20 min. One exception was S which exhibited significant diffusion even at 600°C. This result suggests that external source diffusion will not be viable in GaN due to very low diffusivities of the dopant species. The lack of redistribution of most of these dopants was later verified up to 1100°C [89].

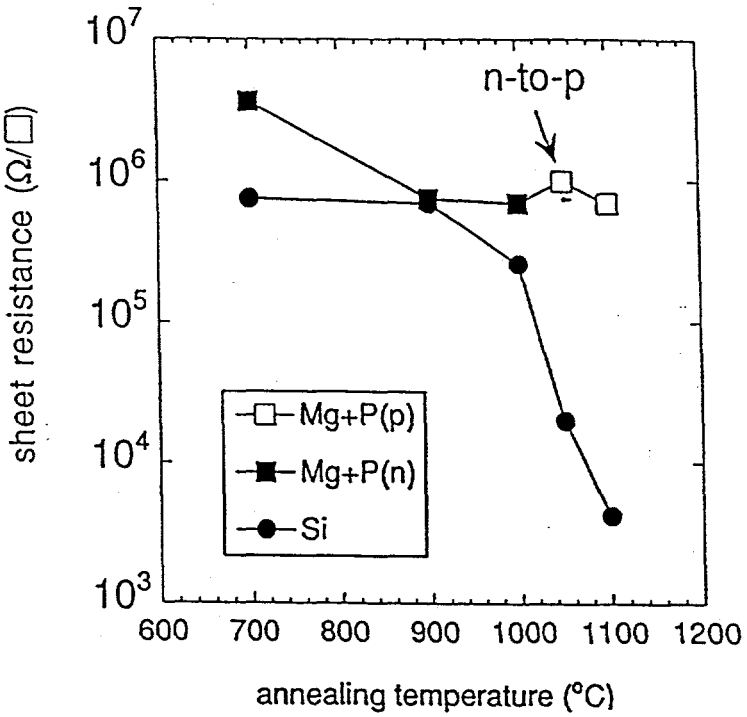

Figure 9. Sheet resistance versus annealing temperature for Si-implanted or Mg+P implanted GaN. Significant electrical activation of the dopants, as demonstrated by the drop in sheet resistance for the Si-samples and a conversion from n-type to p-type for the Mg+P samples, starts to occur at 1050°C with increased activation at 1100°C. Unimplanted and annealed samples showed a slight decrease in sheet resistance but only from 10^6 to 10^5 Ω/sq.

Turning to the electrical activity of implanted dopants in GaN, Figure 9 shows sheet resistance data versus annealing temperature for Si or Mg+P implanted GaN. These data represent the first report of electrical activity of implanted dopants in GaN [90]. The samples were annealed in a rapid thermal annealer enclosed in a SiC coated graphite susceptor in flowing N_2. The key point from Figure 9 is that electrical activity (a sharp drop in sheet resistance for the Si-implanted samples and a conversion from n-type to p-type for the Mg+P implanted samples) does not occur until 1050°C. At this temperature the GaN film can dissociate by liberating nitrogen; a process

that is accelerated in the presence of hydrogen or water vapor. Therefore, it is critical that the annealing ambient be well controlled to maintain the integrity of the semiconductor. In fact, even when bulk nitrogen loss is not detectable by sputtered Auger Electron Spectroscopy (AES), near surface loss over approximately 50Å can create a degeneratively doped n-type region since N-vacancies are believed to act as donors in GaN [91]. This layer will then enhance ohmic contact formation or degrade Schottky contact properties [92,93]. Control of this surface condition is required for fabrication of transistors incorporating ion implantation since both ohmic and Schottky contacts are required. An effective method to maintain the original surface during the anneal is to encapsulate the GaN surface with a sputter deposited AlN film which can later be removed in a selective KOH-based etch. Using this approach, Pt/Au Schottky contacts have been achieved on GaN after annealing at 1100°C while near ohmic behavior resulted on samples annealed uncapped [93].

Returning to the required implant activation anneal temperature for GaN, Table II contains typical annealing temperature and melting points for GaN and for several other semiconductors. The final column of the table shows the ratio of annealing temperature to melting point. As is the case for GaSb, InP, GaAs and Si, the implant activation temperature generally follows a two-thirds rule with respect to the melting point. For GaN (and SiC, however, the activation temperature presently employed is closer to 50% of the melting point. Therefore, although dopant activation can be achieved in GaN at 1100°C, the optimum annealing temperature may very well be closer to 1700°C to fully remove the implant damage. Since this temperature is beyond the capability of most rapid thermal annealing systems, new annealing apparatus will have to be developed if this temperature is indeed required. This point will be revisited below when the removal of implant damage is examined by channeling Rutherford Backscatterng (C-RBS).

Another important technological tool for which ion implantation is well suited is to explore doping or compensation effects of new species. In the case of GaN, one critical technological issue is the determination of an alternative acceptor species to Mg that has a smaller ionization energy (the ionization energy of Mg is ~170 meV) and therefore would yield more free holes at room temperature. Along these lines, Ca had been suggested as being a shallow acceptor in GaN [94] and ion implantation was used for the first demonstration of p-type GaN based on Ca-doping [95]. Unfortunately, the ionization energy of Ca was also shown to be equivalent to that of Mg; however, this result demonstrates the utility of ion implantation for introducing various species into the semiconductor host to study their properties.

Turning now to the build-up and removal of implant damage in GaN, Figure 10 shows channeling C-RBSA spectra for Si-implanted GaN at various doses and after an annealing treatment. Figure 10a demonstrates the GaN has a very high threshold of amorphization, on-the-order-of $2x10^{16}cm^{-2}$, where amorphization is taken as the point where the implanted spectrum coincides with the random spectrum [96]. This is in contrast to GaAs where an amorphous region forms for room temperature implants near a dose of $4x10^{13}cm^{-2}$ but is similar to high Al-fraction AlGaAs which is not amorphized until a similar dose is achieved [96]. Typically in other III-V semiconductors, if amorphization is avoided during the implantation process, most of the damage can be removed during the implant activation anneal with the semiconductor returned near to the pre-implant damage level. However, Figure 10b shows that even for a Si-implant dose of $5x10^{15}cm^{-2}$ that does not amorphize the sample, significant damage, well above the unimplanted level, remains after a 1100°C, 15 sec anneal [97]. This supports the hypothesis that higher temperature annealing will be required to optimize the implant activation process. Recent results have shown, however, at least for Si-implantation in GaN, that even in the presence of significant residual implant damage high dopant activation efficiencies and low resistance regions can be obtained [97].

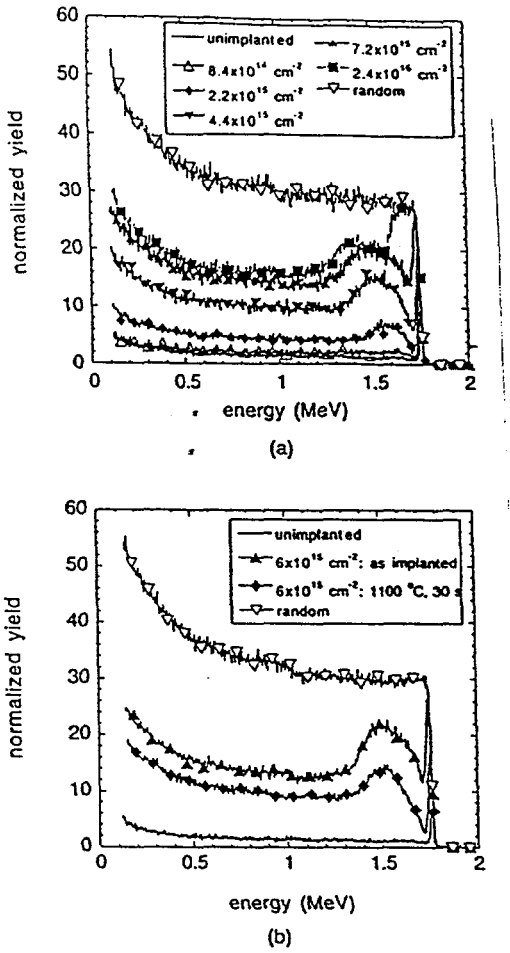

Figure 10. Channeling Rutherford Backscattering spectra for Si-implanted GaN at an energy of 100 keV a) for various Si-doses and B) for a dose of $6x10^{15}cm^{-2}$ both as-implanted and after a 1100°C, 30 sec anneal. The spectra in (a) demonstrates the high threshold of amorphization of GaN during implantation while the spectra in (b) demonstrates that significant damage remains in high dose Si-implanted GaN even after annealed at 1100°C.

A final area of implantation process of compound semiconductors is the formation of select areas of high resistance material for inter-device isolation or current guiding. For both n- and p-type GaN, N-implantation is effective for introducing compensating point defects [90]. This approach yielded a maximum sheet resistance after annealing in the range of 750 to 850°C where the implantation-induced defect density is partially removed to reduce defect assisted hopping conduction but still sufficient to compensate the extrinsic epitaxial doping [90]. Additional work has shown that He is also an effective isolation species for n-type GaN while H-implantation has limited utility for isolation since the compensation anneals out below 400°C [98]. The fact that H-implantation isolation is not effective is not clearly understood but may relate to the implanted hydrogen acting to passivate the compensating point defects during the low temperature anneal. Finally, implantation isolation of In-containing III-nitride materials has shown that InGaN, as used in a LED, laser cavity, or transistor channel, can not be rendered highly resistive by F or O-implantation while InAlN can be highly compensated by O- or N-implants [99-101].

The utility of ion implantation for fabricating the variety of high power device structures, eg. MOS-controlled thyristor, MOS Turnoff thyristor, insulated gate bipolar transistor, necessary for power switching will depend largely on the ability of the crystal growers to produce thick

(>10μm), lightly doped ($n<10^{15}cm^{-3}$) GaN layers, and high-resistivity substrates.

Table II: Comparison of semiconductor melting points (T_{mp}) with the temperature required to activate implanted dopants (T_{act}).

	T_{mp}(°C)	T_{act}(°C)	T_{act}/T_{mp}
GaSb	707[a]	500-600	0.77
InP	1057[a]	700-750	0.69
GaAs	1237[A]	750-900	0.69
Si	1410[a]	950	0.67
SiC	2797[a]	1300-1600	0.46-0.57
GaN	2518[b]	~1100	0.44

[a]Handbook of Chemistry and Physics, ed. Robert C. Weast, (CRC Press, Boca Raton, FL, 1983) p. E-92-93.
[B]J.A. Van Vechten, Phys. Rev. B, 7, 1479 (1973).

Casady and Johnson [7] have recently reviewed implantation in SiC technology. Boron has proven to have higher activation than Al and in most cases the implant is performed at 700-800°C to avoid amorphization. The activation annealing is performed at 1100-1650°C under Ar ambients.

SUMMARY AND CONCLUSIONS

There are still numerous technical obstacles to optimizing the performance of wide bandgap semiconductor devices, including

(i) improved ohmic contacts to p-GaN. One potential solution here is grading to p-InGaN of the highest In concentration that will allow achievement of p-doping, and which is consistent with the requisite thermal stability of the device. The higher the In composition the lower this thermal stability will be, but the specific contact resistivity will also be improved. This solution may favor MBE and MOMBE over MOCVD, because of their lower growth temperatures and ability to incorporate higher In concentrations in InGaN.

(ii) improved trench etching and laser mesa etching processes for SiC and GaN, respectively. Optimization of ICP and ECT plasma chemistries and conditions should be sufficient, and LE4 may play a role because of its potentially lower damage. In this respect, the availability of slow, controlled wet etch processes for damage clean-up after dry etching is also desirable.

(iii) high temperature (>500°C) stable Schottky contacts to GaN for power transistors - WN_x should be explored in this context.

(iv) the availability of high quality gate oxides for MOS devices in both GaN and SiC. While SiO_2 works adequately in many cases on SiC, more development is needed, and there is little systematic work reported for AlN or Ga_2O_3 on GaN. The latter has produced exciting results on GaAs in recent times, but its thermal stability may be an issue on GaN.

ACKNOWLEDGMENTS

The work at UF is partially supported by NSF-DMR (DMR9421109, L.D. Hess), and DARPA (A. Husain) through AFOSR (G.L. Witt). The work at SNL is supported by USDOE (contract DE-AC04-94AL85000). SNL is a multi-program laboratory operated by Sandia Corporation, a unit of Lockheed Martin.

REFERENCES

1. L.S. Rea, Mat. Res. Soc. Vol. 423, 3 (1996).
2. K. Reihardt, J.D. Scofield, and W.C. Mitchel, Proc. Workshop on High Temperature Electronics for Vehicles, eds. G. Khalil, H. Singh, and T. Podlesak, ARL Tech. Rep., pp. 73-79, April 1995.
3. D.M. Brown, E. Downey, M. Ghezzo, J. Krechmer, V. Krishanmurty, W. Hennessy, and G. Michon, Sol. State Electronics, 39, 1543 (1996).
4. J. Palmour, J.S. King, D. Waltz, J. Edmond, and C. Carter, Trans. 1st Intl. High Temperature Conference, Albuquerque, NM, pp. 207-212 (1991).
5. A.K. Agarwal, R.R. Seirgeij, S. Seshadri, M.H. White, P.D. McMullin, A.A. Burk, L.B. Roland, C.D. Brandt, and R.H. Hopkins, Mat. Res. Soc. Symp. 423, 87 (1996).
6. M. Bhatnagar and B.J. Baliga, IEEE Trans. Electron. Dev. 40, 645 (1993).
7. J.B. Casady and R.W. Johnson, Sol. State Electronics 39, 1409 (1996).
8. See for example GaN and related materials ed. F. Ponce, R.D. Dupuis, J.A. Edmond, and S Nakamura, MRS Vol. 395 (1996) and references therein.
9. H.H. Han, J.S. Williams, J. Zou, D.J.H. Cockayne, S.J. Pearton, and R.A. Stall, Appl. Phys. Lett. 69, 2364 (1996).
10. J.C. Zolper, D.J. Reiger, A.G. Baca, S.J. Pearton, J.W. Lee, and R.A. Stall, Appl. Phys. Lett. 69, 538 (1996).
11. L.M. Porter, R.F. Davis, J.A. Bow, M.J. Kim, and R.W. Carpenter, J. Mater. Res. 10, 26 (1995).
12. J. Crofton, P.A. Barnes, J.R. Williams, and J.A. Edmond, Appl. Phys. Lett. 62, 384 (1993).
13. N. Lundberg and M. Ostling, Solid-State Electronics 39, 1559 (1996).
14. N. Lundberg, Ph.D. Thesis, Royal Inst. Technology, Sweden (1996).
15. F. Ren, in GaN and Related materials, ed. S.J. Pearton (Gabon and Breach, NY, 1997).
16. F. Ren, C.R. Abernathy, S.J. Pearton, and P.W. Wisk, Appl. Phys. Lett. 64, 1508 (1994).
17. F. Ren, C.R. Abernathy, S.N.G. Chu, J.R. Lothian, and S.J. Pearton, Appl. Phys. Lett. 66, 1503 (1995). F. Ren. S.J. Pearton, J.R. Lothian, S.N.G. Chu, W.K. Chu, R.G. Wilson, C.R. Abernathy, and S.S. Peri, Appl. Phys. Lett. 65, 2165 (1994).
18. M.E. Lin, Z. Ma, F.Y. Huang, Z.F. Fan, L.H. Allen, and H. Morkoc, Appl. Phys. Lett. 64, 1003 (1994).
19. M.E. Lin, F.Y. Huang, and H. Morkoc, Appl. Phys. Lett. 64, 2557 (1994).
20. A. Durbha, S.J. Pearton, C.R. Abernathy, J.W. Lee, P.H. Holloway, and F. Ren, J. Vac. Sci. Technol. B14, 2582 (1996).
21. M.W. Cole, D.W. Eckart, W.Y. Han, R.L. Pfeffer, T. Monahan, F. Ren, C. Yuan, R.A. Stall, S.J. Pearton, Y. Li, and Y. Lu, J. Appl. Phys. 80. 278 (1996).
22. C.R. Abernathy, J.D. MacKenzie, S.R. Bharatan, K.S. Jones, and S.J. Pearton, Appl. Phys. Lett. 66, 1632 (1995).
23. F. Ren, S.J. Pearton, S. Donovan, C.R. Abernathy, and M.W. Cole, ECS Proc. Vol. 96-11, 122 (1996).
24. C.B. Vartuli, S.J. Pearton, C.R. Abernathy, J.D. MacKenzie, R.J. Shul, J.C. Zolper, M.L. Lovejoy, A.G. Baca, and M. Hagerott-Crawford, Mat. Res. Soc. Symp. Vol. 421, 373 (1996); J. Vac. Sci. Technol. B14, 3520 (1996).
25. S.M. Donovan, J.D. MacKenzie, C.R. Abernathy, C.B. Vartuli, S.J. Pearton, F. Ren, M.W. Cole, and K. Jones, Mat. Res. Soc. Symp. Proc. 449, 771 (1997).

26. L.F. Lester, J.M. Brown, J.C. Ramer, L. Zhang, S.D. Hersee, and J.C. Zolper, Appl. Phys. Lett. 69, 2737 (1996).
27. Z. Fan, S.N. Mohammad, W. Kim, O. Aktas, A.E. Botcharev, and H. Morkoc, Appl. Phys. Lett. 68, 1672 (1996).
28. B.P. Luther, S.E. Mohney, T.N. Jackson, M.A. Khan, Q. Chen, and J.W. Wang, Appl. Phys. Lett. 70, 57 (1997).
29. D.B. Ingerly, Y.A. Chang, N.R. Perkins, and T.F. Kuech, Appl. Phys. Lett. 70, 108 (1997).
30. S. Nakamura, M. Senoh, and T. Mukai, Appl. Phys. Lett. 62, 2390 (1993).
31. S. Nakamura, M. Senoh, and T. Mukai, Jpn. J. Appl. Phys. 30, L1708 (1991).
32. S.C. Binari, L.B. Rowland, W. Kruppa, G. Kelner, K. Doverspike, and D.K. Gaskill, Electron Lett. 30, 1248 (1994).
33. M.A. Khan, M.S. Shur, and Q. Chen, ibid., 31, 2130 (1995).
34. M.A. Khan, J.N. Kuznia, A.R. Bhattarai, and D.T. Olson, Appl. Phys. Lett. 62, 1248 (1993).
35. S. Nakamura, M. Senoh, and T. Mukai, ibid., 62, 2390 (1993).
36. I. Akasaki, H. Amano, M. Kito, and K. Kiramatsu, J. Lumin. 48/49, 666 (1991).
37. S. Nakamura, M. Senoh, N. Iwasa, and S. Nagahama, Appl. Phys. Lett. 67, 1868 (1995).
38. J.C. Zolper, A.G. Baca, R.J. Shul, R.G. Wilson, S.J. Pearton, and R.A. Stall, ibid., 68, 1266 (1996).
39. S. Nakamura, M. Senoh, S. Nagahama, N. Iwasa, T. Yamada, T. Matsushita, H. Kiyoku, and Y. Sugimoto, Jpn. J. Appl. Phys. 35, L74 91996).
40. I. Adesida, A. Mahajan, E. Andideh, M. Asif Khan, D.T. Olsen, and J.N. Kuznia, Appl. Phys. Lett. 63, 2777 (1993).
41. M.E. Lin, Z.F. Zan, Z. Ma, L.H. Allen, and H. Morkoc, ibid., 64, 887 (1994).
42. A.T. Ping, I. Adesida, M. Asif-Khan, and J.N. Kuznia, Electron. Lett. 30, 1895 (1994).
43. H. Lee, D.B. Oberman, and J.S. Harris, Jr., Appl. Phys. Lett. 67, 1754 (1995).
44. S.J. Pearton, C.R. Abernathy F. Ren, J.R. Lothian, P.W. Wisk, A. Katz, and C. Constantine, Semicond. Sci Technol. 8, 310 (1993).
45. S.J. Pearton, C.R. Abernathy, and F. Ren, Appl. Phys. Lett. 64, 2294 (1994).
46. L. Zhang, J. Ramer, K. Zheng, L.F. Lester, and S.D. Hersee, Paper presented at MRS Fall Meeting, Boston, MA (1995).
47. R.J. Shul, S.P. Kilcoyne, M. Hagerott-Crawford, J.E. Parameter, C.B. Vartuli, C.R. Abernathy, and S.J. Pearton, Appl. Phys. Lett. 66, 1761 (1995).
48. R.J. Shul, S.J. Pearton, and C.R. Abernathy, Abstract 311, p. 412, The Electrochemical Society Meeting Abstracts, Vol. 96-1, Los Angeles, CA, May 5-10, 1996.
49. C.B. Vartuli, S.J. Pearton, J.W. Lee, J. Hong, J.D. MacKenzie, C.R. Abernathy, and R.J. Shul, Appl. Phys. Lett. 69, 1426 (1996).
50. K.M. Taylor and C. Lenie, J. Electrochem. Soc. 107, 308 (1960).
51. G. Long and L.M. Foster, J. Am Ceram. Soc. 42, 53 (1959).
52. N.J. Barrett, J.D. Grange, B.J. Sealy, and K.G. Stephen, J. Appl. Phys. 57, 5470 (1985).
53. C.R. Aita and C.J. Gawlak, J. Vac. Sci. Technol. A1, 403 (1983).
54. G.R. Kline and K.M. Lakin, Appl. Phys. Lett. 43, 750 (1983).
55. T. Pauleau, J. Electrochem. Soc. 129, 1045 (1982).
56. T.Y. Sheng, Z.Q. Yu, and G.J. Collins, Appl. Phys. Lett. 52, 576 91988).
57. J.R. Mileham, S.J. Pearton, C.R. Abernathy, J.D. MacKenzie, R.J. Shul, and S.P. Kilcoyne, ibid., 67, 1119 (1995).
58. Q.X. Guo, O. Kato, and Y. Yoshida, This Journal, 139, 2008 (1992).

59. C.B. Vartuli, S.J. Pearton, J.W. Lee, C.R. Abernathy, J.D. MacKenzie, J.C. Zolper, R.J. Shul, and F. Ren, J. Electrochem. Soc. 143, 3681 (1996).
60. M.S. Minsky, M. White, and E.L. Hu, Appl. Phys. Lett. 68, 1531 91996).
61. J.S. Shor and R.M. Osgood, J. Electrochem. Soc. 140, L123 (1993).
62. C. Youtsey, I. Adesida, and G. Bulman, Electronics Lett. (in press).
63. H.P. Gillis, D.A. Choutov, and K.P. Martin, J. Mater., August 1996, pp. 50-55.
64. G.F. McLane, S.J. Pearton, and C.R. Abernathy, Wide Bandgap Semiconductors and Devices, Vol. 95-21 (ECS, Pennington, NJ), pp. 204-214.
65. R.J. Shul, G.B. McClellan, S.A. Casalnuovo, D.J. Rieger, S.J. Pearton, C. Constantine, C. Barratt, and R.K. Karlicek, Appl. Phys. Lett. 69, 1119 (1996).
66. S.J. Pearton, J.W. Lee, J.D. MacKenzie, C.R. Abernathy, and R.J. Shul, Appl. Phys. Lett. 67, 2329 (1995).
67. F. Ren, J.R. Lothian, Y.K. Chen, J.D. MacKenzie, S.M. Donovan, C.B. Vartuli, C.R. Abernathy, J.W. Lee, and S.J. Pearton, J. Electrochem. Soc. 143, L217 (1996).
68. R.J. Shul, J.C. Zolper, M.H. Crawford, R.T. Hickman, R.D. Briggs, S.J. Pearton, J.W. Lee, R. Karlicek, C. Tran, C. Constantine, and C. Barratt, ECS Prod. Vol. 96-15, 232 (1996).
69. H.P. Gillis, D.A. Choutov, K.P. Martin, S.J. Pearton, and C.R. Abernathy, J. Electrochem. Soc. 143, L251 (1996).
70. R.T. Leonard and S.M. Bedair, Appl. Phys. Lett. 68, 794 (1996).
71. J.R. Flemish, K. Xie, and G.F. McLane, Mat. Res. Soc. Symp. Proc. 428, 106 (1996).
72. A.J. Steckl and P.H. Yih, Appl. Phys. Lett. 60, 1966 (1992).
73. J.W. Palmour, R.F. Davis, T.M. Wallett, and K.B. Bhashin, J. Vac. Sci. Technol. A. 4, 590 (1986).
74. J.B. Casady, E.D. Luckowski, M. Bozack, D. Steridan, R.W. Johnson, and J.R. Williams, Tech. Dig. Of Int. Conf. SiC Related materials, Kyoto, Japan 1995, pp. 382-383.
75. P.H. Yih and A.J. Steckl, J. Electrochem. Soc. 140, 1813 (1993).
76. J.R. Flemish, Proc. Widebandgap Semiconductors and Devices, ed. F. Ren (Electrochemical Society, Pennington, NJ 1995) Vol. 10, pp. 231-235.
77. J.R. Flemish, K. Xie, and J.H. Zhao, Appl. Phys. Lett. 64, 2315 (1994).
78. J.R. Flemish, K. Xie, W. Buchwald, L. Casas, J.H. Zhao, G.F. McLane, and M. Dubey, Mat. Res. Soc. Symp. Proc. 339, 145 (1994).
79. J.B. Casady and R.W. Johnson, Solid State Electron. 39, 1409 (1996); J.B. Casady, E.D. Luckowski, M. Bozack, D. Sheridan, R.W. Johnson, and J.A. Williams, J. Electrochem. Soc. 143, 750 (1996).
80. S.J. Pearton, J.W. Lee, J.M. Grown, M. Bhaskaran, and F. Ren, Appl. Phys. Lett. 68, 2987 (1996).
81. C.B. Vartuli, S.J. Pearton, C.R. Abernathy, J.D. MacKenzie, E.S. Lambers, and J.C. Zolper, J. Vac. Sci. Technol. B14, 3523 (1996).
82. O. Ambacher, M.S. Brandt, R. Dimitrov, T. Metzger, M. Stutzmann, R.A. Fischer, A. Miehr, A. Bergmaier, and G. Dollinger, J. Vac. Sci. Technol. B14, 3532 (1996).
83. J.H. Edgar, Properties of Group III Nitrides (INSPEC IEEE London 1994).
84. J.I. Pankove and J.A. Hutchby, J. Appl. Phys. 47, 5387 (1976).
85. H. Amano. M. Kito, K. Hiramatsu, and I. Akasaki, Jap. J. Appl. Phys. 28, L2118 (1989).
86. S. Nakamura, T. Mukai, M. Senoh, and N. Iwasa, Jap. J. Appl. Phys. 31, L139 (1992).
87. J.W. Lee, S.J. Pearton, J.C Zolper, and R.A. Stall, Appl. Phys. Lett. 68, 2102 (1996).

88. R.G. Wilson, C.B. Vartuli, C.R. Abernathy, S.J. Pearton, and J.M. Zavada, Solid-State Elec. 38, 1329 (1995).
89. J.C. Zolper, M. Hagerott-Crawford, S.J. Pearton, C.R. Abernathy, C.B. Vartuli, J. Ramer, S.D. Hersee, C. Yuan, and R.A. Stall, Mat. Res. Soc. Symp. Proc. Vol. 394, 801 (1996).
90. S.J. Pearton, C.R. Abernathy, C.B. Vartuli, J.C. Zolper, C. Yuan, and R.A. Stall, Appl. Phys Lett. 67, 1435 (1995).
91. H.P. Maruska and J.J. Tietjen, Appl. Phys. Lett. 15, 327 (1969).
92. L.F. Lester, J.M. Brown, J.C. Ramer, L. Zhang, S.D. Hersee, and J.C. Zolper, Appl. Phys. Lett. 69, 2737 (1996).
93. J.C. Zolper, D.J. Rieger, A.G. Baca, S.J. Pearton, J.W. Lee, and R.A. Stall, Appl. Phys. Lett. 69, 538 (1996).
94. S. Strite, Jpn. J. Appl. Phys. 33, L699 (1994).
95. J.C. Zolper, R.G. Wilson, S.J. Pearton, and R.A. Stall, Appl. Phys. Lett. 68, 1945 (1996).
96. H.H. Tan, J.S. Williams, J. Zou, D.J.H. Cockayne, S.J. Pearton, and R.A. Stall, Appl. Phys. Lett. 69, 2364 (1996).
97. J.C. Zolper, M.H. Crawford, J.S. Williams, H.H. Tan, and R.A. Stall, Conf. Proc. Of Ion Beam Modification of Materials, 1-6, 1996, Albuquerque, NM (in press).
98. S.C. Binari, H.B. Dietrich, G. Kelner, L.B. Rowland, K. Doverspike, D.K. Wickenden, J. Appl. Phys. 78, 3008 91995).
99. S.J. Pearton, C.R. Abernathy, P.W. Wisk, W.S. Hobson, and F. Ren, Appl. Phys. Lett. 63, 1143 (1993).
100. J.C. Zolper, S.J. Pearton, C.R. Abernathy, C.B. Vartuli, Appl. Phys. Lett. 66, 3042 (1995).
101. J.C. Zolper, M. Hagerott-Crawford, S.J. Pearton, C.R. Abernathy, C.B. Vartuli, C. Yuan, and R.A. Stall, J. Electron. Mat. 25, 839 (1996).